

# Static and Dynamic Energy Absorption of Al Foams Produced by a Sintering and Dissolution Process

D.X. SUN and Y.Y. ZHAO

This article investigates the effects of the processing conditions of the novel sintering and dissolution process (SDP), including sintering temperature, sintering time, Mg addition, and cell size, on the capacities of the as-processed Al foams for static and dynamic energy absorption. While higher temperatures generally promote better bonding between the Al particles during sintering and, therefore, improved energy-absorption capacities, there exist optimum sintering times and cell-size ranges for producing Al foams with the best energy-absorption characteristics. The optimum sintering time increases when the sintering temperature or the relative density is decreased. The addition of a small amount of Mg powder to the Al/NaCl compact can enhance the sintering markedly and increase the energy-absorbing capacity of the foam by up to 50 pct. For any Al foam, the energy absorbed in the static condition is much greater than that in the dynamic condition. The mechanisms of these effects are also discussed.

## I. INTRODUCTION

AL foams have found increasing applications in many areas, including fortifying building and transport structures against buckling and impact, as heat exchangers, and as sound absorbers, owing to their exceptional properties.<sup>[1,2,3]</sup> The properties of an Al foam are primarily determined by the composition of the matrix material and the relative density as well as topology of the cells, which varies considerably for different manufacturing methods. The microstructure of the foam matrix is largely determined by the form of the Al in processing. While the foam made by a liquid-route method is generally free of impurities in the cell walls or struts, the foam made by a solid-route method may incorporate considerable amounts of oxides and other defects in the cell walls. The morphology of the cells of the foam is, however, mainly determined by the foaming agent used. The Al foams made by gas injections into the Al melt or decomposition of gas-releasing particles in the Al melt have soap-bubble-like polyhedral closed cells.<sup>[4]</sup> The Al foams made by casting the Al melt in an unleachable negative mold or by pressure infiltration of the Al melt into a leachable particle compact have open cells formed by a network of thin struts. The Al foams made by decomposition of gas-releasing particles in an Al powder compact have closed cells with relatively thick walls. The foams made by the sintering and dissolution process (SDP) have open cells with rough walls, a combination different from any of the aforementioned foams. The commercial foams currently available have shown a wide range of mechanical properties.<sup>[4]</sup> To evaluate the effectiveness of the Al foam for energy absorption under static and dynamic conditions, the manufacturing method and its conditions need to be taken into account.

The SDP is a novel process for manufacturing Al foams, which was developed at the University of Liverpool.<sup>[5]</sup> The SDP consists of mixing, compacting, and sintering of Al

and NaCl powder mixtures and final dissolution of the NaCl. It is a relatively low-cost process for manufacturing open-cell Al foams because of the inexpensive raw materials and simple process equipment. The cell sizes and porosities of the Al foams made by the SDP can be controlled accurately by selecting appropriate NaCl particles and by specifying the proportions of Al and NaCl in the compacts, because the morphology and sizes of the cells are virtually replicas of those of the NaCl particles. The porosity of the foams is usually in the range of 50 to 85 pct. The microstructural and mechanical characteristics of the foams made by this route are considerably different from those made by the other commercial methods and need to be investigated.

The mechanical properties and the energy-absorption properties of the foams made by the SDP are predominately determined by the sintering process, *i.e.*, the sintering temperature and time. If the sintering temperature is above the melting point of Al, the molten Al tends to separate from the NaCl particles. If the sintering temperature is too low, however, the sintering may take too long to achieve sufficient bonding. If the sintering time is too long there may be severe oxidation of the Al particles, resulting in poor bonding. If the sintering time is too short, however, the bonding between the Al particles is weak. Therefore, there exist optimum sintering temperature and time ranges for each Al/NaCl mixture.

The compaction process in the SDP also has a significant effect on the subsequent sintering. Al particles usually form a highly protective amorphous oxide layer about 3-nm thick at room temperature. The thickness of the oxide film can grow to 20 to 30 nm when the temperature approaches 650 °C.<sup>[6]</sup> The oxide film formed on the surface of the Al particles during atomization and subsequent handling is a big problem for the sintering of the Al powder. During compaction, the oxide films are ruptured at the points where the particles are in contact with each other. As a consequence, the local contacts between the Al particles are fresh and the diffusion of the Al atoms through these contacts is enhanced. Thus, the higher the compaction pressure, the more effective the subsequent sintering operation.<sup>[7]</sup> However, the rupture of the oxide films during compaction is insufficient for ensuring

D.X. SUN, Postdoctoral Student, and Y.Y. ZHAO, Lecturer, are with the Department of Engineering, University of Liverpool, L69 3GH, Liverpool, United Kingdom. Contact e-mail: d.sun@liv.ac.uk

Manuscript submitted April 23, 2002.

strong sintering.<sup>[8]</sup> The oxide films cannot be ruptured completely, and even if they could be, they would remain entrapped in the compacts. Furthermore, new oxide layers will continue to form at the surfaces of the Al particles if any amount of air exists in the compact during the sintering at a high temperature around the melting point of Al.

Mg powder has previously been used in the sintering of Al powders to reduce the oxide film of the Al particles, because the free energy of formation of its oxide is lower than that of Al. A small amount of Mg powder was found to be sufficient to facilitate effective diffusion and sintering.<sup>[8-12]</sup> It is natural to presume that the sintering of Al/NaCl compacts could also be enhanced by the addition of Mg powder in the compacts.

Cell sizes in the foams may also have a big effect on the static and dynamic energy absorption. Although a wide range of Al foams have recently become available, investigations of the effect of cell size on energy absorption are still lacking. This is partly because of the fact that these foams have low controllability of cell-size ranges. The cells of the foams made by the SDP, however, can vary from 100  $\mu\text{m}$  to 10 mm and can be controlled relatively accurately. The foams are ideal for the investigations of the effect of cell size on the energy absorption of open-cell Al foams.

This article studies the effects of the SDP processing conditions such as sintering temperature, sintering time, Mg addition, and cell size on the static and dynamic energy-absorption characteristics of the resultant foams, with an aim to optimize the SDP for producing Al foams with desired porosities.

## II. EXPERIMENTAL

The precursor materials used in this study were a commercially pure gas-atomized Al powder, a commercial NaCl powder, and a commercially pure Mg powder, with particle sizes in the ranges of 100 to 400, 150 to 3000, and 200 to 500  $\mu\text{m}$ , respectively. In the study of the effects of sintering temperature and time, the Al powder was mixed with the NaCl powder with the proportion of NaCl in the range of 20 to 70 wt pct. In the study of the effects of Mg additions the Al powder was mixed with the Mg powder and the NaCl powder, with the proportion of Mg in the range of 0 to 0.6 wt pct and a fixed proportion of NaCl of 70 wt pct. In the study of the effect of cell sizes, the NaCl powder was further divided into six size groups: 150 to 250, 340 to 420, 500 to 600, 710 to 800, 1200 to 1500, and 2400 to 3000  $\mu\text{m}$ . The Al powder was first mixed with the Mg powder and, subsequently, with the NaCl powder in each size group separately. The proportions of Mg and NaCl in these specimens were fixed at 0.15 and 70 wt pct, respectively. The powder mixtures were then compacted under a pressure of 200 MPa using an hydraulic press. The compacts, contained in sealed steel molds in order to separate them from the air atmosphere, were sintered in an electrical furnace at a temperature of 600  $^{\circ}\text{C}$  to 650  $^{\circ}\text{C}$  for a time of 2 to 110 hours. After the specimens cooled to room temperature, they were removed from the furnace and placed into a hot flowing-water bath of  $\sim 95$   $^{\circ}\text{C}$  and kept for 2.5 to 6 hours to dissolve the NaCl particles in the compacts.<sup>[13]</sup> The as-obtained foam specimens were finally annealed at 550  $^{\circ}\text{C}$  for 0.5 hours to relieve the residual stresses.

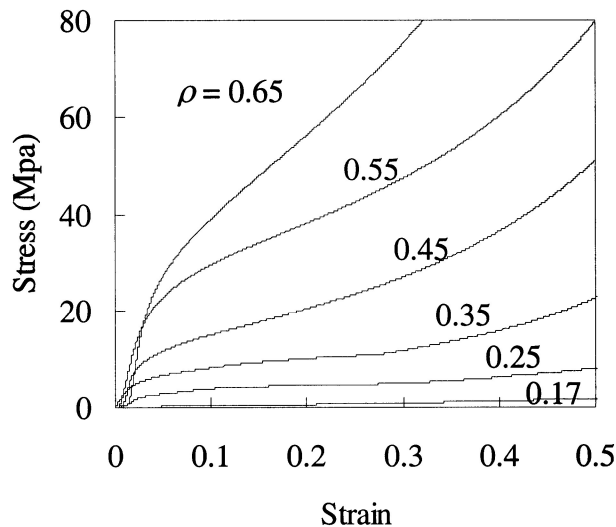


Fig. 1—Compressive stress-strain curves for Al foams with different relative densities.

All the foam specimens for mechanical tests were ground into a cylindrical shape with a cross-sectional area of 1102.5  $\text{mm}^2$  and a height of 30 mm, which was chosen to be at least 10 times larger than the cell diameters to minimize the scatter of the data.<sup>[14]</sup> The quasi-static compressive tests were carried out on an Instron 4505 mechanical tester with a strain rate of  $1.6 \times 10^{-2}$   $\text{mm s}^{-1}$ . The impact tests were carried out in an impact tower, with an impactor of 4 kg falling from a height of 0.5 m, equivalent to a total impact energy of 20 J. The velocity of the impactor was  $3.1 \times 10^3$   $\text{mm s}^{-1}$  when it impacted the surface of the specimen. Less than 5 pct of the stored energy was consumed by the friction on the carriage. The impact force and the velocity of the impactor were measured by a piezoelectric load cell and a Flowlite laser Doppler velocimeter, respectively, with an interval time of 0.043 ms. An Hitachi S-2460N scanning electron microscope with energy-dispersive spectroscopy (EDS) capability was used to observe the microstructures and to analyze the chemical compositions of the foams.

## III. RESULTS AND DISCUSSIONS

### A. Sintering Temperature and Time

Figure 1 shows the typical compressive stress-strain curves for the Al foams, with relative densities ( $\rho$ ) ranging from 0.17 to 0.65 and with no Mg addition, as produced in the SDP with a sintering temperature ( $T$ ) of 650  $^{\circ}\text{C}$  and a sintering time ( $t$ ) in the range of 2 to 30 hours. The relative density is the ratio of the densities between the foam and the bulk Al. The compressive strength of the Al foam at any fixed strain increases nearly proportionally with increasing relative density. The curves are very smooth as compared with those of the foams produced by most other manufacturing methods. This indicates that the cell structure of the Al foams made by the SDP is very uniform.

Figure 2 shows the variations of the absorbed energy of the Al foams at a nominal strain of 0.3 in the compressive tests with the square root of sintering time for producing the Al foams, at different sintering temperatures and relative

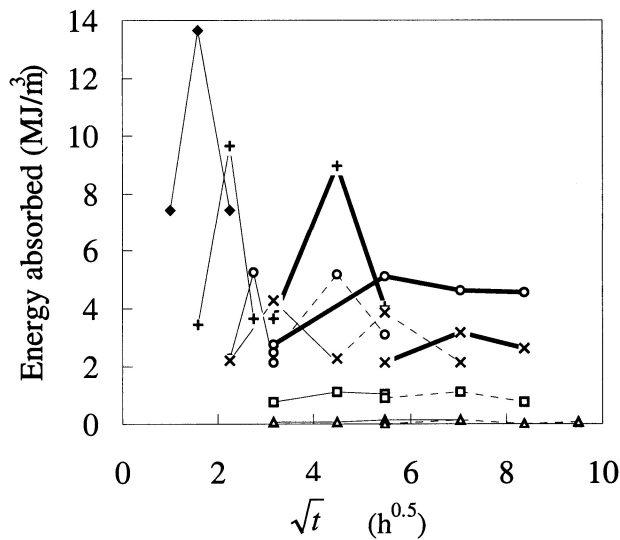


Fig. 2—Variations of absorbed energy of Al foams at a strain of 0.3 with sintering time for different sintering temperatures and relative densities.

densities. The sintering temperature and the relative foam density corresponding to each curve are shown by the designated line and the symbol, respectively. It is shown that for any Al foam with a fixed sintering temperature, there exists an optimum sintering time at which the foam has a maximum energy absorption. At a sintering temperature of 650 °C, the optimum sintering times are 2.5, 5, 7.5, 10, 20, and 30 hours for obtaining Al foams with relative densities of 0.65, 0.55, 0.45, 0.35, 0.25, and 0.17, respectively. At 630 °C, the optimum sintering times are 20, 30, 50, and 50 hours to obtain foams with relative densities of 0.45, 0.35, 0.25, and 0.17, respectively. At 610 °C, the times are 20, 30, and 50 hours to obtain relative densities of 0.55, 0.45, and 0.35, respectively.

The sintering temperature has been found to be the most critical parameter for producing Al foams in the SDP. As the sintering process is diffusion controlled, higher temperatures promote better bonding between adjacent Al particles. The lower the sintering temperature, the longer the sintering time needed to achieve sufficient bonding. When the sintering temperature is below 600 °C, Al foams cannot be made even after a long sintering time of 110 hours.

The proportion of NaCl in the Al/NaCl compacts is also an important parameter. At a fixed sintering temperature, the optimum sintering time increases with an increasing proportion of NaCl in the compacts. NaCl has a much lower thermal conductivity than Al, with the former being  $6.49 \text{ W m}^{-1} \text{ K}^{-1}$  and the latter being  $235 \text{ W m}^{-1} \text{ K}^{-1}$ . Therefore, the more NaCl in the Al/NaCl compact, the lower the overall thermal conductivity. The sintering time must be increased when more NaCl is present in the compacts in order to ensure sufficient heating in the interior regions of the compacts. The proportion of NaCl in the Al/NaCl compacts is usually controlled in the range of 50 to 80 wt pct. When it is higher than 80 wt pct, it is difficult to produce a foam because there is not a sufficient connection between the Al particles. When it is lower than 50 wt pct, a large number of the NaCl particles will be enclosed by the surrounding Al particles and, thus, be trapped in the resultant foam.

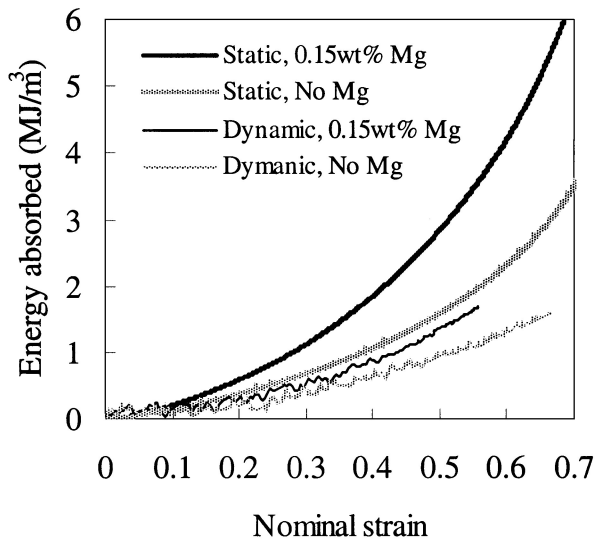
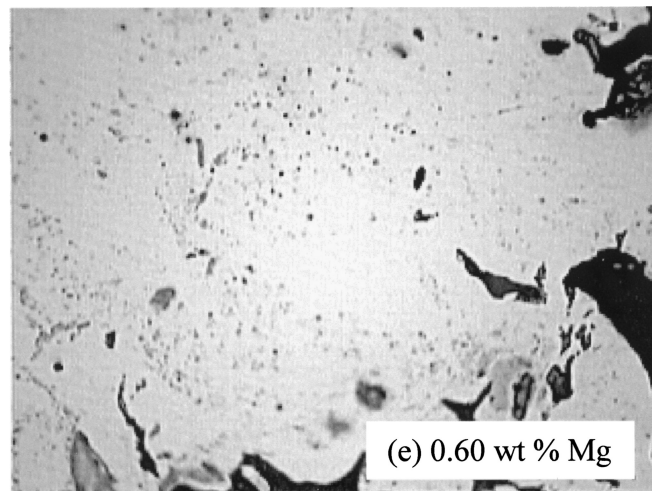
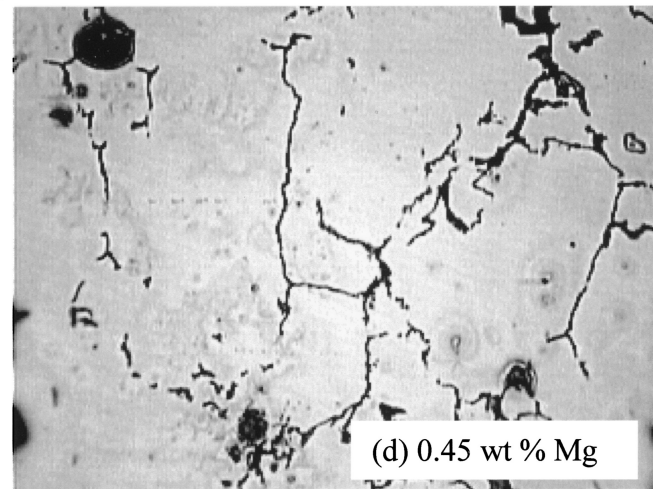
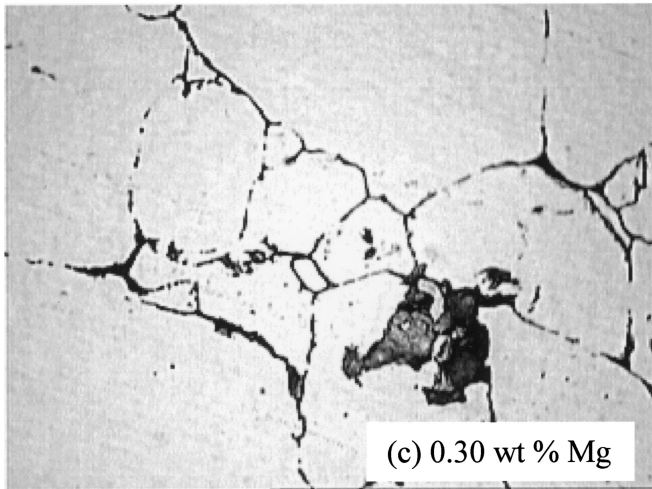
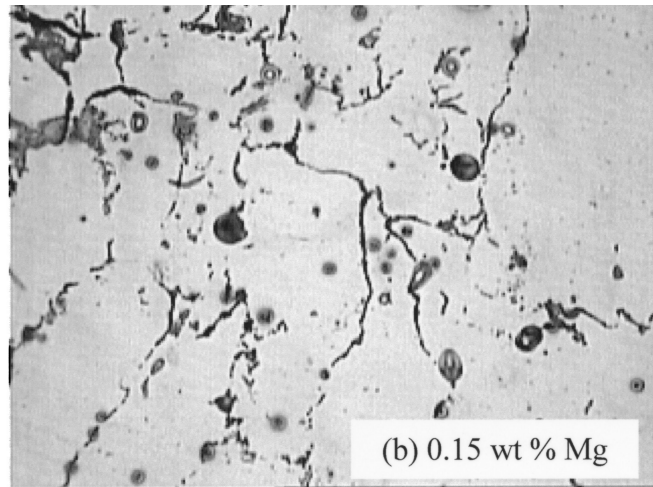
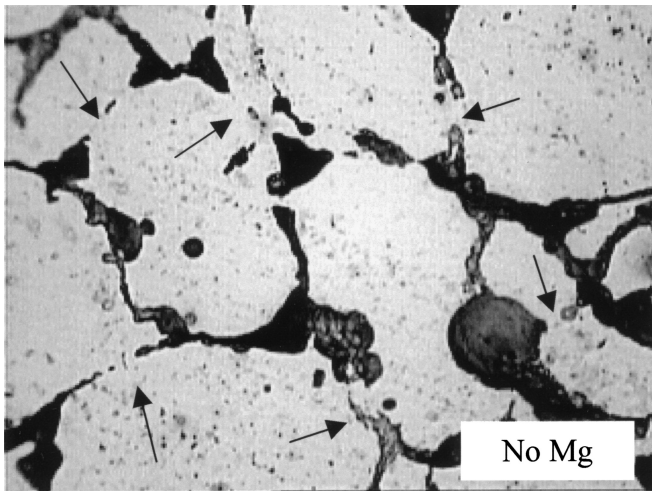


Fig. 3—Variations of static and dynamic energy absorption with nominal strain for Al foams with a relative density of 0.25, with or without Mg addition.

### B. Magnesium Addition

Figure 3 shows the variations of static and dynamic energy absorption with nominal strain in the compressive and impact tests for the Al foams produced by sintering at 650 °C for 20 hours. The foams have a relative density of 0.25 and cell sizes of 710 to 800  $\mu\text{m}$  with either no Mg addition or 0.15 wt pct of Mg, which is equivalent to 0.5 wt pct of the weight of the foam. The energy absorbed by the foams with the addition of Mg is nearly 50 pct greater than that without Mg in either the static or dynamic test. For the foams produced under the same conditions, the energy absorbed in the static tests is much greater than that in the dynamic tests, with the former being nearly twice the latter. Similar results have been found in the compressive and impact tests for the foams that have a relative density of 0.25 and cell sizes of 150 to 250, 340 to 420, 500 to 600, 1200 to 1500, and 2400 to 3000  $\mu\text{m}$ , respectively. It has been demonstrated that the strength of the foams is increased significantly by the addition of a relatively small amount of Mg in the Al/NaCl compacts.

Figure 4 shows typical optical micrographs of the cell walls in the Al foams produced by sintering at 650 °C for 20 hours, with a relative density of 0.25 and with the additions of different amounts of Mg. When no Mg is added, as shown in Figure 4(a), the Al particles are largely surrounded by the dark regions, which are believed to be oxides formed at the surfaces of the particles. It can be seen that there is severe oxidation of the Al particles during the sintering without the addition of Mg. The strength of the foam is low because there are only limited bonding regions between the Al particles, as pointed out by the arrows. The amount of oxides at the boundaries between the Al particles is reduced markedly with increasing Mg additions, as shown in Figures 4(b) through (e). On the other hand, relatively large dark regions are found to scatter in the cell walls. They are believed to be the oxides of Mg,  $\text{MgAl}_2\text{O}_4$ , and MgO, formed at the locations of the original Mg particles. The EDS spectra of the boundary regions between the Al particles in the foams with no Mg or 0.15 wt pct of Mg, as shown in



100  $\mu\text{m}$

Fig. 4—Optical micrographs of the cell walls in the Al foams with a relative density of 0.25 and different amounts of Mg additions: (a) 0, (b) 0.15, (c) 0.3, (d) 0.45, and (e) 0.6 wt pct.

Figure 5, confirm that the amount of oxygen decreases with increasing Mg additions.

There have been extensive studies on the oxidation behavior of Al alloys containing Mg.<sup>[15–18]</sup> The oxidation rate of

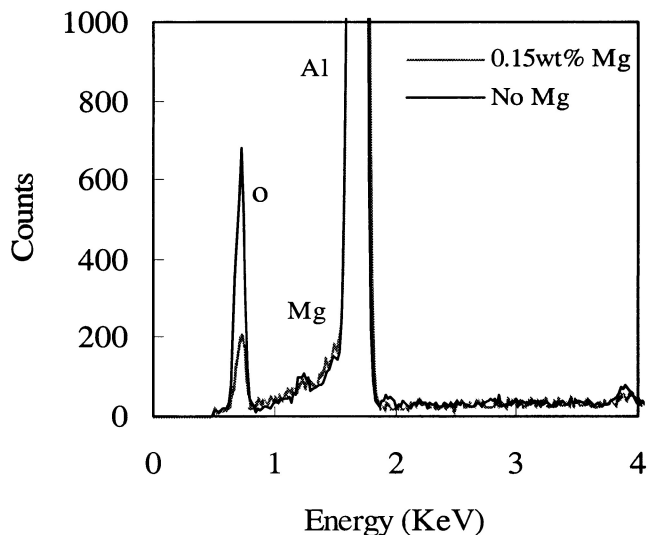


Fig. 5—EDS spectra showing different O levels in the interparticle boundary regions in the Al foams with or without Mg addition.

Al-Mg alloys is much higher than that of the pure Al,<sup>[15]</sup> and the oxide layers are invariably composed of  $MgAl_2O_4$  and  $MgO$ , any of which can be the dominant constituent.<sup>[16,17]</sup>  $MgAl_2O_4$  is thermodynamically favored and often predominates in the oxide layers.<sup>[15,16]</sup>  $MgO$  has a higher growth rate and may predominate in certain cases, especially at relatively high Mg concentrations.<sup>[17]</sup> Secondary  $MgAl_2O_4$  crystallites can also form by the reduction of the amorphous  $Al_2O_3$  layer existing before the oxidation.<sup>[17]</sup>

The enhancement of the sintering of Al powder by the addition of Mg in the form of elemental powder is mainly due to the disruption of the  $Al_2O_3$  layer at the surfaces of the Al particles, allowing improved diffusion bonding between the particles.<sup>[8-12]</sup> However, the mechanism of the reduction process is less clear. Lumley *et al.*<sup>[8]</sup> proposed that the reduction of  $Al_2O_3$  is mainly realized by the diffusion of Mg along the metal-oxide interface and through the Al particles, facilitated by the Al-Mg contacts formed as a consequence of the local oxide rupture during compaction. The product of the reduction reaction was found to be  $MgAl_2O_4$ , although  $MgO$  was assumed to form where Mg is in direct contact with  $Al_2O_3$ . They also found that there is an optimum Mg concentration for each powder, which increases with the total volume of the oxide surface layers and, thus, decreases with the particle size of the Al particles. The optimum Mg concentration for one powder was 0.15 wt pct, which was 3 times that calculated to allow for complete reduction of the  $Al_2O_3$ . The excessive Mg was considered to be required for reacting with the lubricant added to the compact.<sup>[8]</sup>

The effect of Mg in the SDP is likely to be in the following two aspects. First, there is always small amount of air trapped in the Al/NaCl compact. Without the existence of Mg in the compact, the air can lead to significant oxidation of the Al particles during the sintering. When Mg is present in the compact, however, the air will mostly be absorbed by the Mg, because of the preferential oxidation of Mg. The contacts between the Al particles at which the oxide films have been ruptured during compaction would remain intact during sintering, without further oxidation. Second, the existent oxide

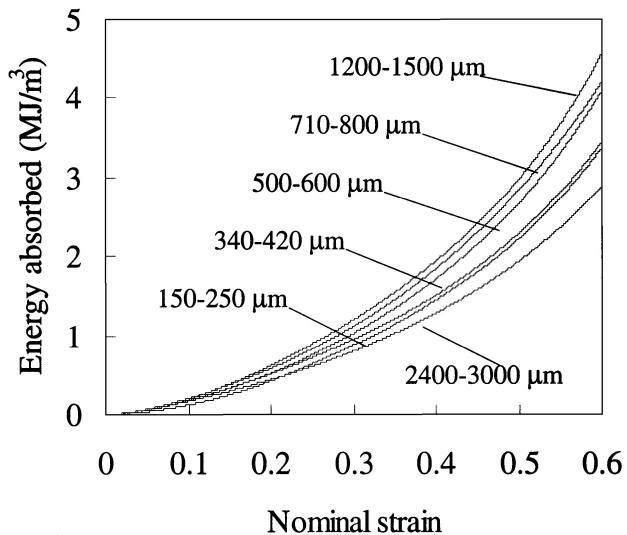


Fig. 6—Variations of absorbed energy with nominal strain in compressive tests for Al foams with a relative density of 0.25 and different cell sizes.

films of the Al particles are reduced directly by the Mg particles, leading to an improved sintering response. However, it seems unlikely that the dominant paths of the diffusion of Mg are through the Al particles, as proposed by Lumley *et al.*<sup>[8]</sup> The compaction of the Al/NaCl compact cannot guarantee the formation of large areas of intimate contact between the Mg and Al particles. Because the proportion of Mg in the compact is very small and the Mg particles are sparsely distributed, effective diffusion of Mg in the Al matrix would require intimate contact not only between the Mg particles and the surrounding Al particles, but also between the successive Al particles throughout the Al matrix. The diffusion of Mg through the large amount of interface among the Al particles is likely to make a greater contribution to the transport of Mg to the sites of the oxide films.

### C. Cell Size

Figure 6 shows the variations of energy absorption with nominal strain in the compressive tests for Al foams with different cell-size ranges, produced by sintering at 650 °C for 20 hours with the addition of 0.15 wt pct Mg. The foams have a relative density of 0.25 and cell sizes of 150 to 250, 340 to 420, 500 to 600, 710 to 800, 1200 to 1500, and 2400 to 3000  $\mu m$ , respectively. The energy absorbed by the foam increases steadily with increasing nominal strain until the densification point, as expected. At a fixed strain, the energy absorbed by the foam increases by increasing the cell sizes of the foams, up to 1500  $\mu m$ . However, it decreases with cell sizes further increased to 2400 to 3000  $\mu m$ .

Figure 7 shows the variations of the energy absorption with nominal strain in dynamic tests for Al foams with different cell-size ranges, produced by sintering at 650 °C for 20 hours with the addition of 0.15 wt pct Mg. The foams have a relative density of 0.25 and cell sizes of 150 to 250, 340 to 420, 500 to 600, 710 to 800, 1200 to 1500, and 2400 to 300  $\mu m$ , respectively. The energy absorbed by the foam increases serratedly with the nominal strain until all the input energy is absorbed. At a fixed strain, the energy absorbed by the foam increases with increasing cell sizes of the foams,

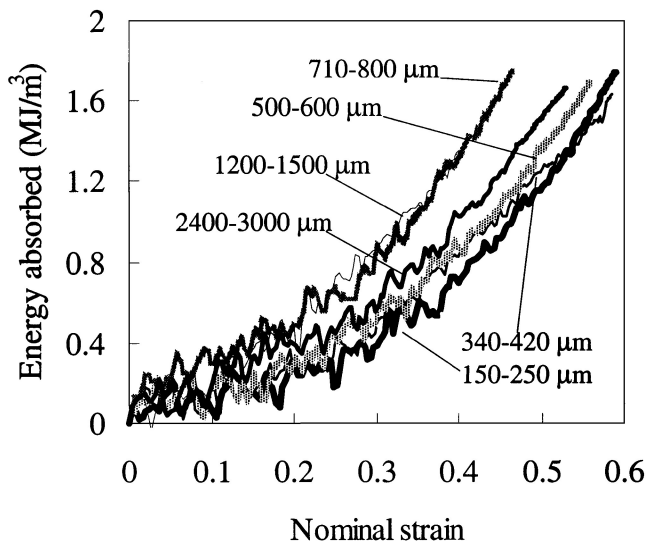


Fig. 7—Variations of absorbed energy with nominal strain in dynamic tests for Al foams with a relative density of 0.25 and different cell sizes.

up to 800  $\mu\text{m}$ . However, it decreases with increasing cell sizes. It can be seen from Figures 6 and 7 that there is an optimum cell-size range in which the foam absorbs the maximum amount of energy in both static and dynamic tests. The optimum size ranges are 1200 to 1500  $\mu\text{m}$  in the static tests and 710 to 800  $\mu\text{m}$  in the dynamic tests.

The effect of cell sizes on energy absorption can be understood by considering their effect on the strength of the Al foams. As mentioned previously, the morphology and sizes of the cells are virtually replicas of those of the NaCl particles. For a fixed Al/NaCl ratio in the compact, the smaller the NaCl particles, the larger the total interfacial area between the Al matrix and the NaCl particles. As a consequence, there is likely to be more air trapped in the compact, which can lead to more severe oxidation. A simple geometric analysis can show that the amount of air trapped in the compact is, approximately, inversely proportional to the NaCl particle size. The relative amounts of the trapped air and, therefore, the relative amounts of oxide corresponding to the particle-size ranges of 150 to 250, 340 to 420, 500 to 600, 710 to 800, 1200 to 1500, and 2400 to 3000  $\mu\text{m}$  are 13.5, 7.1, 4.9, 3.6, 2, and 1, respectively. Therefore, the greater the cell sizes, the better the bonding that can be achieved during sintering and, thus, the higher the foam strength. When the NaCl particles are large enough, however, the amount of trapped air becomes small and does not vary much. The optimum bonding can be achieved in sintering, leading to the strongest foam. If the cells are too big, however, some cell walls may become too thin relative to the cell sizes. These thin cell walls are more likely to buckle under a lower compressive pressure. More research is needed for a better mechanistic understanding of this effect.

#### IV. CONCLUSIONS

In the SDP, the processing conditions such as sintering temperature, sintering time, Mg addition, and cell size have

significant effects on the static and dynamic energy absorption of the as-processed Al foams. In solid-state sintering, higher temperatures promote better bonding between the Al particles and, therefore, improve energy-absorption characteristics. At a fixed sintering temperature, there is an optimum sintering time for producing an Al foam with a certain relative density. The optimum sintering time increases when the sintering temperature or the relative density is decreased. An addition of Mg powder as little as 0.5 wt pct of the weight of the resultant foam in the Al/NaCl compact can enhance the sintering markedly and increase the energy-absorbing capacity of the foam up to 50 pct. There is also an optimum cell-size range in which the foam absorbs the maximum amount of energy. The optimum cell-size ranges are 1200 to 1500  $\mu\text{m}$  and 710 to 800  $\mu\text{m}$  for static and dynamic energy absorption, respectively. For any Al foam, the energy absorbed in the static condition is much greater than that in the dynamic condition, with the former being as much as twice the latter at any fixed strain.

#### ACKNOWLEDGMENTS

The authors acknowledge the support of a Research Development Fund provided by the University of Liverpool. One of the authors (DXS) thanks the University of Liverpool for a studentship.

#### REFERENCES

1. L.J. Gibson and M.F. Ashby: *Cellular Solids: Structure and Properties*, 2nd ed., Cambridge University Press, Cambridge, United Kingdom, 1997, pp. 8-11.
2. *Metal Foams*, J. Banhart and H. Eifert, eds., Verlag MIT Publishing, Bremen, 1997.
3. *Metal Foams and Porous Metal Structures*, J. Banhart, M.F. Ashby, and N.A. Fleck, eds., Verlag MIT Publishing, Bremen, 1999.
4. M.F. Ashby et al.: *Metal Foams: A Design Guide*, Butterworth-Heinemann, 2000.
5. Y.Y. Zhao and D.X. Sun: *Scripta Mater.*, 2001, vol. 44, pp. 105-10.
6. P.S. Corkish: Ph.D. Thesis, the University of Liverpool, Liverpool, 1976, pp. 1-39.
7. R.M. German: *Powder Metallurgy Science*, Metal Powder Industries Federation, NJ, 1984, pp. 119-26.
8. R.N. Lumley, T.B. Sercombe, and G.B. Schaffer: *Metall. Mater. Trans. A*, 1999, vol. 30A, pp. 457-63.
9. A.P. Savitskii and L.S. Martaunova: *Poroshk. Metall.*, 1977, vol. 173 (5), pp. 14-19.
10. A.B. Al'tman, V.A. Brodov, A.V. Zhil'tsov, and I.P. Melashenko: *Poroshk. Metall.*, 1987, vol. 297 (9), pp. 713-17.
11. N.S. Timofeev and A.P. Savitskii: *Poroshk. Metall.*, 1990, vol. 327 (3), pp. 20-25.
12. G.B. Schaffer, T.B. Sercombe, R.N. Lumley, and S.H. Huo: in *Powder Metallurgy Aluminum & Light Alloys for Automotive Applications*, A. Russell et al., eds., MI, 2000, pp. 11-18.
13. D.X. Sun, T. Fung, and Y.Y. Zhao: in *Cellular Metals and Metal Foaming Technology*, J. Banhart, M.F. Ashby, and N.A. Fleck, eds., Verlag MIT Publishing, Bremen, 2001, pp. 237-40.
14. T. Mukai, H. Kanahashi, T. Miyoshi, M. Mabuchi, T.G. Nieh, and K. Higashi: *Scripta Mater.*, 1999, vol. 40 (8), pp. 921-27.
15. G.M. Scamans and E.P. Butler: *Metall. Trans. A*, 1975, vol. 6A, pp. 2055-63.
16. H.P. Leighly, Jr. and A. Alam: *J. Phys. F: Met. Phys.*, 1984, vol. 4, pp. 1573-83.
17. M.H. Zayan, O.M. Jamjoom, and N.A. Razik: *Oxid. Met.*, 1990, vol. 34, pp. 323-33.
18. D.H. Kim and E.P. Yoon: *J. Mater. Sci.*, 1996, vol. 5, pp. 1429-31.